ACS APPLIED MATERIALS & INTERFACES

Research Article

www.acsami.org

Citrate-Capped Silver Nanoparticles Showing Good Bactericidal Effect against Both Planktonic and Sessile Bacteria and a Low Cytotoxicity to Osteoblastic Cells

Constanza Y. Flores, Alejandro G. Miñán, Claudia A. Grillo, Roberto C. Salvarezza, Carolina Vericat,* and Patricia L. Schilardi*

Instituto de Investigaciones Fisicoquímicas Teóricas y Aplicadas (INIFTA), Facultad de Ciencias Exactas, UNLP, CCT La Plata, CONICET, CC16 Suc 4 (1900), La Plata, Argentina

ABSTRACT: A common problem with implants is that bacteria can form biofilms on their surfaces, which can lead to infection and, eventually, to implant rejection. An interesting strategy to inhibit bacterial colonization is the immobilization of silver (Ag) species on the surface of the devices. The aim of this paper is to investigate the action of citrate-capped silver nanoparticles (AgNPs) on clinically relevant Gram-positive (*Staphylococcus aureus*) and Gram-negative (*Pseudomonas aeruginosa*) bacteria in two different situations: (i) dispersed AgNPs (to assess the effect of AgNPs against planktonic bacteria) and (ii) adsorbed AgNPs on titanium (Ti) substrates, a material widely used for implants (to test their effect against sessile bacteria). In both cases, the number of surviving cells was quantified. The small amount of Ag on the surface of Ti has an antimicrobial effect similar to that of pure Ag surfaces. We have also investigated the capability of AgNPs to kill planktonic bacteria and their cytotoxic effect on UMR-106 osteoblastic cells. The minimum bactericidal concentration found for both strains is much lower than the AgNP concentration that leads to cytotoxicity to osteoblasts. Planktonic *P. aeruginosa* show a higher susceptibility to Ag than *S. aureus*, which can be caused by the different wall structures, while for sessile bacteria, similar results are obtained for both strains. This can be explained by the presence of extracellular polymeric substances in the early stages of *P. aeruginosa* biofilm formation. Our findings can be important to improving the performance of Ti-based implants because a good bactericidal action is obtained with very small quantities of Ag, which are not detrimental to the cells involved in the osseointegration process.

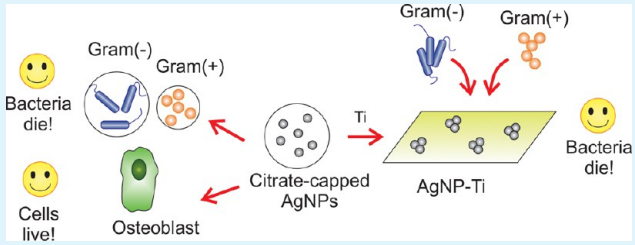

KEYWORDS: *silver nanoparticles, antibacterial effect, titanium substrates, biofilm, planktonic bacteria, cytotoxicity, osteoblasts*

INTRODUCTION

A common problem with implants and other implantable medical devices is that bacteria can form biofilms on their surfaces, which can lead to local or systemic infections and, eventually, to implant rejection. This is a major worry for both patients and health care providers because of the negative impact in the quality of life of the former and the economical cost of frequent implant replacements.[1] An interesting strategy to inhibit bacterial colonization is the immobilization of an antibacterial agent on the surface of the devices that can inhibit the adhesion of pioneer bacteria and kill them as they try to attach to the surface. It is well-known that bacteria that form biofilms are more resistant to antimicrobial agents added after colonization of the surface.[2]

Silver (Ag) compounds have been used as antimicrobial agents since a long time ago, and nowadays, with the advent of nanomaterials, different types of silver nanoparticles (AgNPs) and Ag-containing nanocomposites have been proposed to try to circumvent the menace of biofilm formation. Ag, in the form of either ions or AgNPs, is a broad spectrum bactericidal that lacks the resistance problems that some antibiotics present. Moreover, Ag and its compounds are effective virucidal[3] and antifungal[4] agents. Thus, the use of adsorbed AgNPs or other Ag species on the surface of implants and medical supplies is a valid strategy to hinder the formation of biofilms and hence the incidence of infections. In this respect, surfaces modified by Ag nanomaterials have been proven to have antibacterial properties against different bacterial strains.[5−7]

Several strategies have been developed to immobilize Ag nanomaterials on different surfaces, most of them including one or more surface functionalization steps.[8,9] For instance, in materials such as glass and stainless steel, functionalization of the substrate surface, usually with self-assembled monolayers of organic molecules, is needed for efficient Ag nanomaterial adsorption.[5,6] Apart from surface substrate modification, because of their antimicrobial properties, AgNPs are also used in a wide range of products, such as cosmetics and fabrics, among others.[7] For instance, Lee et al.[10] have developed a procedure for producing nanosized stable Ag particles on

Received: January 5, 2013
Accepted: March 27, 2013
Published: March 27, 2013

cotton fabrics that inhibit the growth of various bacteria without side effects on the skin.

Though highly effective against bacteria, the mechanism of action of AgNPs against them is not yet fully understood: while some authors attribute their antibacterial effect to the release of Ag ions, others state that it is due to the interaction of AgNPs with the walls of the cells and still others propose a combination of both effects.[11−18]

Several studies have been performed to assess the effect of AgNPs on both Gram-positive and Gram-negative planktonic bacteria. In some of them, minimum bactericidal or inhibitory concentrations (MBC and MIC, respectively) have been reported.[19−21] Because the release of Ag ions from the nanoparticles is certainly involved in diminution of the bacterial viability, the size, shape, and capping of AgNPs are important factors to consider. For instance, it has been reported that truncated triangular AgNPs have a better antibacterial performance on *Escherichia coli* than spherical ones, a fact that was attributed to the presence of high-atom-density facets such as (111), which favors the reactivity of Ag.[22] For AgNPs having the same shape, the MBC tested on both Gram-positive and Gram-negative strains increases as the size of the nanoparticles increases.[23] With regards to the AgNP capping, the charge and nature of the species in the AgNP protective layer play an important role and should not be underestimated.[24] However, in many studies, commercial AgNPs are used and the information on the capping is not informed.[19] In each case, upon critical evaluation of MIC and MBC, it is important to take into account not only the capping but also, if the size and shape of the nanoparticles are known, the available surface area exposed to the media. Moreover, the role of the AgNP environment should also be considered.

Titanium (Ti) is a material widely used in implants because of its good mechanical properties and corrosion resistance due to the formation of a thin passivating TiO_2 film, which is also responsible of its biocompatibility.[25] For these reasons, Ti is the metal of choice for dental implants and, though to a lesser extent, for bone replacement (in the latter case, Ti foams are currently being developed).[26] Consequently, the development of new methods for inhibiting bacterial colonization on Ti, and thus reducing the occurrence of infection, is a challenge that would result in a better performance of the implant.

Compared to assays involving planktonic bacteria, fewer studies have been published dealing with sessile bacteria on surfaces of interest for implantable devices modified with AgNPs.[27,28] Among them, Roe et al. proved that catheters coated with AgNPs showed good antibacterial activity against several strains, preventing biofilm formation on the surface.[29] Vasilev et al. used poly(vinyl sulfonate)-coated AgNPs bound onto amine-containing surfaces, which were effective in preventing the attachment of bacteria.[8] In our previous study,[30] we had shown that citrate-capped AgNPs adsorb spontaneously on Ti/TiO_2 surfaces without the need of pretreatments, and we had also demonstrated the bactericidal effect of such modified surfaces. It is thus interesting to compare the bactericidal action of AgNPs on both planktonic and sessile bacteria on surfaces of materials commonly used for implant materials, like Ti/TiO_2 surfaces (ref 30 and references cited therein).

Furthermore, many concerns have arisen regarding harmful effects of AgNPs on human health and on the environment. It has been proposed that AgNPs have potential inflammatory effects and can also cause damage to the genetic material in cells.[31] Oxidative stress has been related to the cytotoxicity of AgNPs because of the fact that they release Ag ions.[32] It has also been reported that cyto- and genotoxicity of AgNPs depend on the dosage of the nanomaterial.[33] Consequently, it is also crucial to know the cyto- and genotoxic effects of AgNPs on the cells involved in the osseointegration process, like osteoblasts,[34] and to find the AgNP concentration range that is high enough to kill the majority of bacteria but that does not considerably affect the cells that will be in contact or close to the implant.

The aim of this paper is to investigate the action of citrate-capped AgNPs on Gram-positive and Gram-negative bacteria in two different situations: (i) dispersed AgNPs (to assess their effect against planktonic bacteria) and (ii) adsorbed AgNPs on Ti substrates, a material widely used for implants (to test them against sessile bacteria). For this purpose, we have used two clinically relevant bacteria: *Pseudomonas aeruginosa* (*P. aeruginosa*; Gram-negative) and *Staphylococcus aureus* (*S. aureus*; Gram-positive). Moreover, we have tested the cytotoxic effect of AgNPs on an osteoblast cell line (UMR-106). Our results show that the MBC found for both strains is much lower than the AgNP concentration that is cytotoxic to osteoblasts. Planktonic *P. aeruginosa* shows a higher susceptibility to Ag than *S. aureus*, which can be caused by the different wall structures, while for sessile bacteria, similar results are obtained for both strains. This result can be explained by the presence of extracellular polymeric substances (EPS) in the early stages of *P. aeruginosa* biofilm formation.

EXPERIMENTAL SECTION

1. Preparation of AgNP-Coated Ti Substrates. AgNPs (diameter ≈ 6 nm, citrate-coated) were prepared as described elsewhere.[30] The method is based on the reduction of $AgNO_3$ by $NaBH_4$ in a sodium citrate containing dissolution. The physicochemical characterization of the nanoparticles and the AgNP-modified Ti (AgNP-Ti) substrates used in this work can be found in ref 30. Briefly, freshly synthesized nanoparticles showed a narrow size distribution of around 6 nm from high-resolution transmission electron microscopy (HRTEM) imaging. After 3 weeks, the size distribution broadened a bit but AgNPs did not aggregate, as revealed also by the position and intensity of the surface plasmon resonance peak at ≈400 nm. The possibility of formation of an oxide layer on their surface was discarded because the X-ray photoelectron microscopy (XPS) Ag 3d peaks could be fitted with a single component corresponding to metallic Ag. No additional components at lower binding energy were necessary for a correct peak fitting. Moreover, HRTEM and electron diffraction results were consistent with a cubic metallic Ag lattice and not with any silver oxides. Therefore, we concluded that our AgNPs are metallic, with a negligible amount of silver oxide on their surface. Additionally, the AgNPs remained unoxidized after several months, as revealed from XPS and TEM measurements.

Circular Ti foils (1 cm diameter) were polished to mirror grade. Then, they were immersed in the AgNP dispersion (3.16×10^{-2} mg/mL, ≈293 μM, expressed as Ag concentration) for 24 h at 4 °C to allow AgNPs be adsorbed onto the surface. The native oxide of Ti in aqueous media is amorphous TiO_2, about 20 nm thick.[35] This oxide layer is probably hydroxylated. Because the isoelectric point of native TiO_2 is 4.5, the surface charge at pH 7 is negative.[36] The AgNP-Ti substrates were rinsed gently with Milli-Q water and dried under a nitrogen flux. As reported before,[30] after this treatment, AgNPs arranged in islands of 100−300 nm in size with average height 80 nm. The average Ag coverage was ≈0.09. It is worth mentioning that clustering is probably caused by the drying process. However, we have prepared the substrates in that way because the potential application of our study would be AgNP-modified Ti dental implants that should be kept dry and sterile on the shelf until implantation.

The nanoparticles remain adsorbed on the Ti surface after rinsing with water and even after 72 h of immersion in the bacterial culture medium. Moreover, the stability of the adsorbed AgNPs is relatively strong because they can be imaged by contact atomic force microscopy (AFM) without removing them with the tip by using relatively soft cantilevers and low applied forces, as we demonstrated in our previous paper.[30] In fact, higher forces (≈400 nN) were necessary to sweep away some of the adsorbed nanoparticles.

Circular Ti foils of the same diameter that had not been exposed to AgNP dispersions were used as controls. Also, circular Ag foils of the same diameter as the Ti substrates were used in order to compare the antimicrobial effect of bulk Ag to that of AgNP-Ti substrates.

2. Bacterial Culture and Microbiocidal Assays. *Planktonic Bacteria.* *P. aeruginosa* (clinical isolate from a patient with cystic fibrosis) and *S. aureus* (ATCC 25923 methycilin sensible) strains were grown on liquid nutrient broth (Merck, Darmstadt, Germany) at 30 °C on a rotary shaker (250 rpm). Bacterial inocula were prepared in 1 mL of nutrient broth by inoculating 10^8 colony-forming units (CFU)/mL of bacteria in a fresh growth medium and grown at 30 °C for 1 h. Because citrate-capped nanoparticles tend to aggregate in standard growth media,[2] the assays were carried out in a rich phosphate-buffered medium containing 5 g/L glucose, 5 g/L mannitol, and 10 g/L glycine in phosphate buffer, pH 7, 0.01 M (from now on, GMP). The inocula were diluted in GMP to have 10^5 CFU/mL of bacteria for viability assays. CFU values were confirmed by plate counting.

Viability Assay for Planktonic Bacteria. In order to investigate the bactericidal effect of dispersed AgNPs on planktonic cells, AgNPs at different final Ag concentrations (0, 0.09, 0.195, 0.39, 0.78, 1.56, 3.125, 6.25, 12.5, 25, 50, 75, and 150 μM) were suspended in a GMP medium. In each case, an appropriate dilution of the bacterial culture (either *S. aureus* or *P. aeruginosa*), grown in nutrient broth, was added to the AgNPs in a GMP medium to reach a final bacterial concentration of 10^5 CFU/mL. Bacteria were left in contact with the AgNPs for 24 h, and then the total number of viable bacteria was quantified by a serial dilution method and plate counting. Control assays (without AgNPs) were performed by plate counting after 24 h of growth in the GMP medium.

This method allowed us to define the bactericidal concentrations of AgNPs against both *P. aeruginosa* and *S. aureus*. The MBC was defined as the lowest concentration of agent (nanoparticles) that kills at least 99.9% of the total bacteria in 24 h.

Sessile Bacteria. *P. aeruginosa* and *S. aureus* strains were grown on liquid nutrient broth at 30 °C on a rotary shaker (250 rpm). Bacterial inocula were prepared in 50 mL by inoculating 10^7 CFU/mL of bacteria in a fresh growth medium and grown up to an exponential phase. Then, the bacterial suspensions were adjusted to $\approx 1 \times 10^8$ CFU/mL in a fresh growth medium and used immediately for inoculation of the substrates. The CFU was confirmed by a viable count. Subsequently, substrates were vertically placed in the bacteria suspension and incubated at 30 °C for 4 h. The substrates with sessile cells were then removed and washed gently by immersion in sterile Milli-Q water in order to remove or detach those cells that were not tightly attached to the surface. Sessile bacteria prepared in this way were used for the assays described below.

Viability Assay for Sessile Bacteria. The number of bacteria adhered to the surface of the substrates was determined by two separate techniques: (a) quantification by serial dilution and plate counting method; (b) viability assays made by using a Live/Dead BacLight Bacterial Viability Kit from Invitrogen.

Serial Dilution Method. For quantification, the adherent bacteria were detached by sonication. To assess the possibility that ultrasound treatment decreased the bacterial viability, we compared the number of planktonic viable *S. aureus* bacteria with and without ultrasound (control) using the plate counting method. Briefly, *S. aureus* ATCC 25923 was grown in nutrient broth at 30 °C and the bacterial suspension was adjusted to 10^7 CFU/mL in a fresh growth medium. Aliquots of 2 mL of the bacterial suspensions were distributed in four glass tubes. Two of them were immersed in an ultrasonic bath. Sonication at 40 kHz with a power output of 160 W was performed at 30 °C for 15 min. Later, the number of bacteria in the sonicated suspension was determined by serial dilution followed by bacterial culture on nutrient agar. Bacterial suspensions in the remaining tubes were used as control assays. These tubes were incubated for 15 min at 30 °C without ultrasound treatment and counted as described above. The number of viable bacteria exposed to ultrasound treatment was $3.75 \pm 0.92 \times 10^7$ CFU/mL, while the control yielded $3.15 \pm 1.63 \times 10^7$ CFU/mL. Thus, our experimental data reveal no significant differences in the number of viable bacteria exposed to ultrasound treatment compared to the control.

On the other hand, incomplete disaggregation of biofilms would underestimate the number of viable sessile cells. However, while we could have some incomplete disaggregation, ultrasonic treatment is a widely used and reliable method to remove and disaggregate biofilms. Bjerkan et al.[37] have demonstrated that sonication efficiently dislodges bacteria (including *S. aureus*) from biofilms generated in vitro on Ti surfaces. Moreover, the sonication procedure is commonly used for enumeration of viable bacteria by the dilution plate method. Currently, one of the most widely used methods for testing the antibiotic susceptibilities of biofilms in clinical diagnostics is the Calgary's Biofilms device (CBD). After exposure of preformed biofilms to antimicrobial agents, sessile cell quantification is conducted by conventional plating after disruption of biofilms by sonication.[38] The CBD was used in relevant pathogenic species such as *P. aeruginosa* ATCC,[39] *S. aureus*, and *Escherichia coli*.[38] Regarding the chosen sonication time for sessile bacteria detachment and biofilm dissagregation (15 min), we tried 15 and 30 min of sonication for *P. aeruginosa* from Ti substrates and found similar results from bacteria plate counting. Therefore, we chose the shorter time for both sessile *P. aeruginosa* and *S. aureus*.

The detachment of all bacteria was confirmed by epifluorescence microscopy with an Olympus BX-51 microscope after the samples were stained with acridine orange. Then, the number of bacteria in the suspension was determined by serial dilution followed by bacterial culture on nutrient agar. A triplicate series of experiments were carried out in each case. Statistical analysis was performed using one-way analysis of variance (ANOVA) to evaluate differences between groups of bacteria. A $p < 0.05$ was considered statistically significant.

Live/Dead Kit. For *P. aeruginosa*, the staining dissolution was prepared by mixing 30 μL of component A (SYTO 9) and 30 μL of component B (propidium iodide) and diluting the mixture to 1/200 in distilled water. For *S. aureus*, the staining dissolution was prepared by mixing 3 μL of staining component A and 3 μL of staining component B and diluting to 1/1000 in distilled water. A total of 10 μL of the mixture was poured on each substrate, and then they were kept in the dark for 15 min at room temperature. After that, the substrates were rinsed with sterile water. Stained bacteria were visualized by epifluorescence microscopy. The filters used were U-MWG2 (excitation 510−550 nm; emission 590 nm), which allows imaging of intact and damaged bacteria as green cells, and U-MWB2 (excitation 460−490 nm; emission 520 nm), which allows imaging damaged bacteria as red cells. The percentage of bacterial survival was calculated from the ratio of the number of intact cells (green cells minus red cells) to the total number of cells (green cells). Calculations were made from at least 10 different randomly selected regions of each image, by using *Image J* software (National Institute of Health, Bethesda, MD). A triplicate series of experiments were carried out in each case. Statistical analysis was performed using one-way ANOVA to evaluate the differences between groups of bacteria. A $p < 0.05$ was considered statistically significant.

3. Cell Culture. Rat osteosarcoma derived cells (UMR-106 cell line) were originally obtained from American Type Culture Collection (ATCC; Rockville, MD). Cells were grown as a monolayer in Falcon T-25 flasks with a complete culture D-MEM medium (D-MEM medium, high glucose, with L-glutamine, with pyridoxine hydrochloride from GIBCO-BRL, Grand Island, NY, supplemented with 10% inactivated fetal calf serum, 50 IU/mL penicillin and 50 μg/mL streptomycin sulfate) at 37 °C in 5% CO_2 humid atmosphere. Cells were counted in an improved Neubauer hemocytometer, and viability was determined by the exclusion Trypan Blue (Sigma, St. Louis, MO) method. In all cases, the viability was higher than 95%.

Cytotoxicity Evaluation of AgNP in the UMR-106 Cell Line. Two sets of experiments were arranged in order to evaluate the cellular effects of the different AgNP concentrations. Neutral red (NR) and tetrazolium salt (MTT) assays (described below) were carried out using the following concentrations: 10, 25, 50, 75, 100, 150, and 225 μM, each of them corresponding to the final amount of Ag after the addition of the corresponding AgNP aliquot to the different wells. Previously, it had been tested by UV−vis spectroscopy that the citrate-capped AgNPs do not coalesce in the D-MEM culture medium.

NR Assay. The NR uptake assay was performed according to Borenfreund and Puerner.[40] This assay measures cellular transport based on the dye uptake of living cells. Absorbance change is directly proportional to the lysosomal activity of the cells. For this analysis, 2.5×10^3 cells/well (96 multiwell plate) were grown in a complete culture medium for 24 h at 37 °C in a 5% CO_2 humid atmosphere. The culture medium was then replaced by a fresh one with different AgNP concentrations. After exposure, the medium was removed and a fresh medium containing 40 μg/mL NR dye (Sigma, St. Louis, MO) was added. Following 3 h of incubation, cells were washed with a phosphate-buffered saline (PBS) solution. Subsequently, 0.1 mL of a 1% acetic acid solution in 50% ethanol was added. The dye that had been taken by the live cells was released, and the red color was observed. The plate was shaken for 10 min, and the absorbance was measured at 540 nm using an automatic ELISA plate reader (BioTek μQuant). Negative controls were run simultaneously in cultures without AgNPs. The cytotoxicity percentage was calculated as $[(A - B)/A] \times 100$, where A and B are control and treated cell absorbances, respectively. Each experiment was independently repeated three times. Data were analyzed using the one-way ANOVA test, and multiple comparisons were made using p values corrected according to the Bonferroni method.

Reduction of MTT Assay. MTT assay was performed using metabolic competence by the colorimetric method of Mosmann,[41] as modified by Twentyman and Luscombe.[42] This assay measures the reduction of MTT [3-(4,5-dimethylthiazol-2-yl)-2,5-diphenyltetrazolium bromide] to formazan by dehydrogenase enzymes of intact mitochondria in living cells. The absorbance change is directly proportional to the number of viable cells. For this analysis, 2.5×10^3 cells/well (in 96 multiwell plates) were grown in a complete culture medium for 24 h at 37 °C in a 5% CO_2 humid atmosphere. The culture medium was then replaced by a fresh one with different AgNP concentrations. After 24 h, the medium was removed, cells were washed with PBS, and a fresh medium containing MTT reagent (1 mg/mL final concentration; Sigma, St. Louis, MO) was added. After 3 h of incubation, cells were washed again with PBS. Color developed by the addition of 100 μL of dimethyl sulfoxide (Merck, Química Argentina SAIC, Argentina) to each well for cell lysis and formazan crystal dissolution. The plate was shaken for 10 min, and the absorbance was measured at 540 nm using an automatic ELISA plate reader. Each experiment was independently repeated three times. The cytotoxicity percentage and statistical analysis were calculated as described previously for NR assays.

4. Ag Release. Circular AgNP-Ti substrates and Ag foils (both 1 cm in diameter) were placed in separate vials containing 3 mL of Milli-Q water. After 4 h, the substrates were removed and 3 mL of 0.1 M HNO_3 was added to each of the supernatants. The total Ag concentration was then measured by graphite furnace atomic absorption spectrometry.

In order to estimate the Ag release of disperse nanoparticles after 24 h in GMP and D-MEM media, an appropriate aliquot of the AgNP dispersion was added to 20 mL of each medium so as to obtain a final Ag concentration of 5 μM. For comparison, the same procedure was made by replacing the medium by Milli-Q water. After 24 h, the dispersions were ultracentrifuged (Beckman) at 100000g for 2 h, and then the UV−vis spectrum of each sample was measured to determine the absorbance of the typical surface plasmon resonance absorption peak at ≈400 nm. Complete separation of the nanoparticles was achieved after two ultracentrifugation steps, as revealed by the absence of the plasmon absorption peak in the UV−vis spectrum. Then, concentrated HNO_3 was added to the supernatant in order to obtain a final concentration of 0.05 M, and the total Ag concentration was measured by graphite furnace atomic absorption spectrometry.

5. AFM Imaging of Bacteria. The substrates were vertically placed in fresh cultures of *P. aeruginosa* or *S. aureus* at 30 °C for 4 h (nutrient broth; final bacterial concentration ≈ 1×10^8 CFU/mL). Then, the substrates were gently rinsed with sterile water and dried in air. AFM images were acquired in contact mode with a NanoScope V scanning probe microscope (Bruker, Santa Barbara, CA) operating in ambient conditions. Silicon nitride probes (k = 0.58 N/m; Bruker) were used in all measurements. For *P. aeruginosa*, analysis of the wall roughness was made from at least three different images (450 × 450 nm^2 in size) with the *Nanoscope 7.30* software using the *Roughness* tool. The average roughness (w) of the bacterial surfaces was calculated as

$$w = \sum_{i=1}^{n} \left[\frac{(z_i - \bar{z})^2}{N} \right]^{1/2} \quad (1)$$

where N is the number of points considered on the surface, z_i the height of point i on the surface, and $\bar{z}$ the average height of N points.

RESULTS AND DISCUSSION

The action of citrate-capped AgNPs on both Gram-positive and Gram-negative bacteria was investigated in two different situations: for dispersed AgNPs and for adsorbed AgNPs on Ti substrates.

Antibacterial Effect of Dispersed AgNPs on Planktonic Cells. Assays were performed in order to evaluate the effect of AgNPs on the viability of both planktonic *S. aureus* and *P. aeruginosa*. Cell killing should not only produce a faster resolution of infections but also improve the clinical performance, as well as reduce the probability of spreading of the infection. The MBC is one of the clinically relevant parameters[7] to account for the effect of AgNPs on the bacteria. We have performed assays in order to determine the MBC values for our systems. In the case of our AgNPs, because citrate-capped nanoparticles tend to aggregate in standard culture media,[2] experiments were carried out in GMP (see the Experimental Section). The MBC values determined for *S. aureus* and *P. aeruginosa* were 3.12 μM (0.33 μg/mL) and 0.78 μM (0.084 μg/mL), respectively (expressed as the total Ag concentration). These figures are far lower than those reported in the literature for different strains of *S. aureus*[19] and *P. aeruginosa*.[20] In order to assess the suitability of the GMP medium, blank experiments (no AgNPs) were performed after 24 h of growth. Both *S. aureus* and *P. aeruginosa* showed a 10-fold increase in the concentration after 24 h, showing that bacteria continue to grow in the conditions of the assays after 24 h.

It has been reported that the size[43] and shape[22] of AgNPs are parameters that influence their bactericidal capacity. The values of MBC and/or MIC reported in the literature cover a wide range of AgNP concentrations, depending on the experimental conditions.[7,21,44,45] In fact, Lara et al.[20] used nanoparticles of 100 nm diameter and found that the MBC for planktonic *P. aeruginosa* was ≈1×10^4 μg/mL, while Ansari et al.[19] reported values of 12−25 μg/mL for nanoparticles of 5−10 nm diameter for *S. aureus*, although the capping of such commercial nanoparticles was not specified. Because the kinetics of Ag^I release[46] and nanoparticle−surface cell interactions[47] depend on the capping of the nanoparticles, the knowledge of the nature of the AgNP capping is not a minor point. In comparison to those reported in the literature, the low values of the MBC found for our citrate-capped AgNPs indicate a very good bactericidal activity against the two strains assayed in this work.

The mechanism of the antibacterial action of AgNPs is still controversial. Some authors have suggested that it is mainly related to the release of Ag ions from the surface of the nanoparticles, which, in turn, can interact with thiol groups present in bacterial proteins,[24] interfere in DNA replication,[16,48] or affect the respiratory chain.[12] In particular, the release of Ag ions from citrate-stabilized nanoparticles would proceed through oxidation involving dioxygen[13] because the concentration of Ag ions diminishes in anaerobic conditions, therefore decreasing the antimicrobial activity.[17] Sotiriou et al.[14] have found that small AgNPs (less than 10 nm) release more Ag^I ions than larger nanoparticles. This high release can be related to their higher curvature[14] and to the presence of defects, such as kink sites,[49] which facilitate Ag dissolution from the nanoparticle surface. Thus, the low MBC found for our AgNPs compared to other values reported in the literature could be attributed to their size (6 nm in diameter), to the lability of the capping, or both. Further investigation is needed in order to better understand this point.

Moreover, according to our results, *P. aeruginosa* is more susceptible to 6 nm citrate-capped nanoparticles than *S. aureus*. It is still open to discussion whether AgNPs can physically interact with cells, causing disruption of the cell membrane and even penetration of nanoparticles into the cytoplasm.[15,17] Some authors have proposed that AgNPs attach to the cell membrane and penetrate into the cell, causing toxicity through protein/membrane damage and oxidative stress.[18] According to Taglietti et al., Gram-negative microorganisms are more sensitive to AgNP dispersions than Gram-positive bacteria.[15] Indeed, they found by TEM that glutathione-coated AgNPs are able to penetrate into *E. coli* cells but not into *S. aureus* because of the differences in the cell-wall structure for both types of bacteria. In our case, the greater resistance of *S. aureus* compared to *P. aeruginosa* could also be attributed to differences in the bacterial wall.[50] In the case of Gram-positive cells, it is formed by an inner cell membrane and an outer thick layer of peptidoglycan. In contrast, the cell wall in Gram-negative cells presents an inner membrane covered by just a thin layer of peptidoglycan and an outer layer of lipopolysaccharides.[51] Accordingly, the observed difference could be explained because of the fact that the thick layer of peptidoglycan in Gram-positive bacteria acts as a barrier, preventing the action of AgNPs, no matter the mechanism involved (Ag^I ion or AgNP internalization).

Cytotoxicity Assays of Dispersed AgNPs on UMR-106 Osteoblastic Cells. Taking into account the clinical implications of using AgNPs as antimicrobial agents, the question that immediately arises is whether the nanoparticles dosed in the concentration range at which they are effective to kill bacteria can produce harmful effects on cells.[7] In fact, it has been reported that AgNPs can reduce the mitochondrial function and also affect the integrity of cell membranes in macrophages.[52] In addition, AgNPs have been identified as responsible for the production of reactive oxygen species and interruption of ATP synthesis, which, in turn, cause DNA damage.[53] To assess this point, we have tested the effect of AgNP dispersions on UMR-106 osteoblastic cells. To this end, cell cultures were exposed to different AgNP concentrations in a complete D-MEM culture medium. Results from NR assays are summarized in Figure 1. No significant differences were found in cells treated with 10, 25, or 50 μM with respect to untreated controls. Cultures with higher AgNP concentrations showed a significant decrease ($p < 0.001$) in the lysosomal

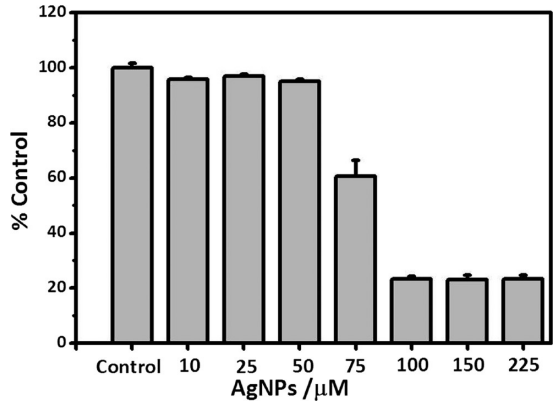

Figure 1. Effect of AgNP-treated UMR-106 cells after 24 h evaluated by NR assay.

activity with respect to the control, reaching values close to 20% of viability (with respect to the controls) for 100, 150, and 225 μM concentrations. Additionally, when cultures were exposed to AgNP concentrations >75 μM, a significant reduction in the mitochondrial activity of cells measured by the MTT test was found ($p < 0.001$) compared to the controls (Figure 2).

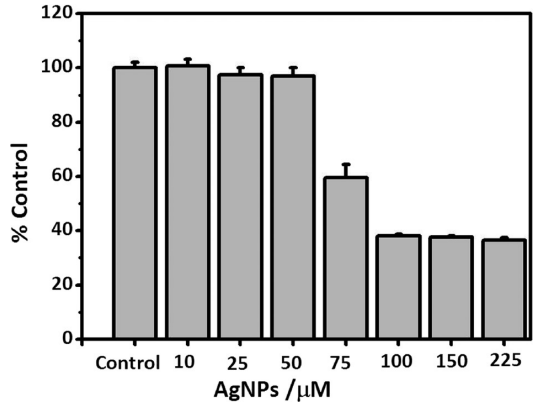

Figure 2. Effect of AgNP-treated UMR-106 cells after 24 h evaluated by MTT assay.

Therefore, our results demonstrate that there is a concentration range for which AgNPs have a detrimental effect on both Gram-positive and Gram-negative bacteria without affecting the viability of the osteoblasts. This result is important because it allows design of the dosage of AgNPs in bone implants in such concentrations that can kill bacteria without significantly affecting the cells involved in the osseointegration process. Although the growth media and other experimental conditions for bacterial and mammalian cell cultures are different, because of the difference in magnitude between the AgNP concentrations that show bactericidal effects for *S. aureus* and *P. aeruginosa* (<4 μM) and that which results in cytotoxicity for UMR-106 osteoblasts (>50 μM), we can conclude that there would be a concentration window that allows the use of AgNPs as antibacterial agents without detrimental effects on the cells surrounding the implants. It is worth mentioning that, the different experimental conditions and markedly different proliferation rate for bacteria and animal cells would make bacterial−eukaryotic cell cocultures unsuitable for cytotoxicity studies.

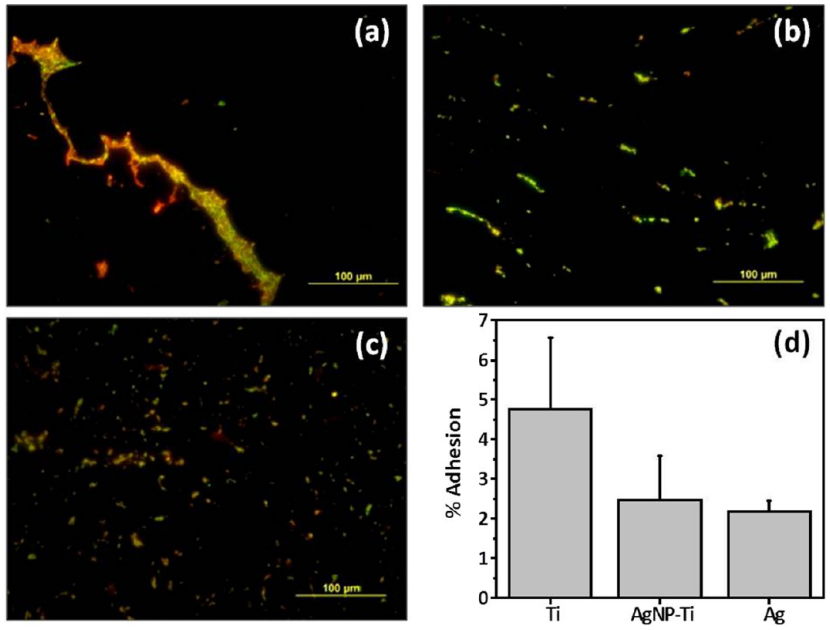

Figure 3. Epifluorescence images of early stages of *P. aeruginosa* biofilm formation on (a) Ti, (b) AgNP-Ti, and (c) Ag. (d) Percentage of adhesion of *P. aeruginosa* on the different substrates.

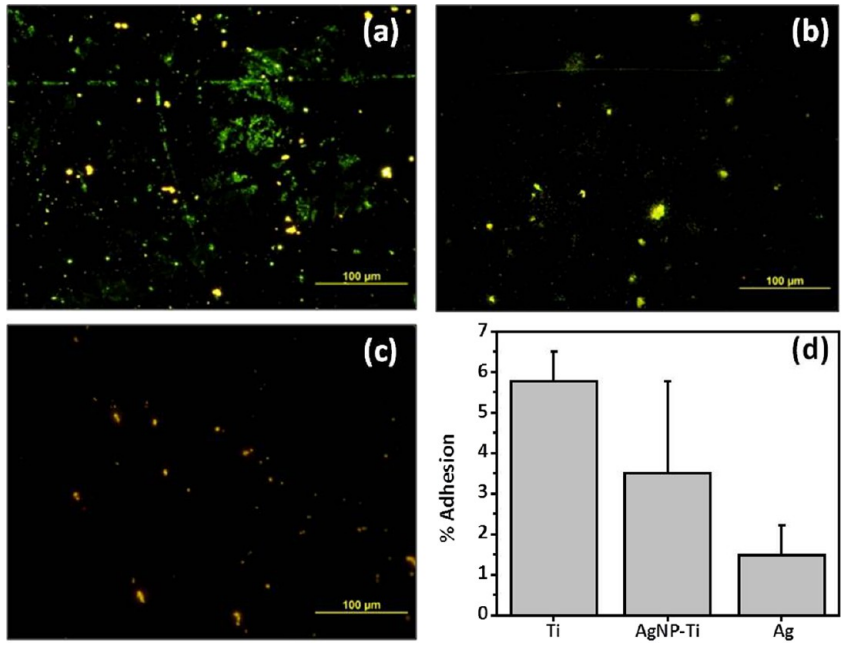

Figure 4. Epifluorescence images of early stages of *S. aureus* biofilm formation on (a) Ti, (b) AgNP-Ti, and (c) Ag. (d) Percentage of adhesion of *S. aureus* on the different substrates.

To assess the role of the two different media used (complete culture D-MEM for osteoblasts and GMP for bacteria), we have tested Ag^I ion release from disperse nanoparticles in both media and compared the results to that obtained in water. In all cases, the initial Ag concentration was 5 μM (0.54 mg/L). After 24 h, the AgNPs were separated by ultracentrifugation and the supernatants were analyzed. The final Ag concentrations were 3, 0.16, and 0.24 μM for water, GMP, and D-MEM, respectively.

The fact that the Ag concentration found in water is higher than that in culture media is in accordance with other authors.[13] The difference between water and the culture media can be explained by taking into account that both GMP and D-MEM contain phosphate ions that can react with Ag^I to form insoluble products. Moreover, D-MEM is a chloride-containing medium, so that part of the released Ag is probably separated from the dissolution by precipitation of silver chloride. Also, Ag ions possibly interact with serum proteins of the complete culture D-MEM medium via carboxylate and thiol groups, and some of these proteins can be eventually separated in the centrifugation step.

Importantly, for a certain initial AgNP concentration, the amount of released Ag in D-MEM is on the same order as that

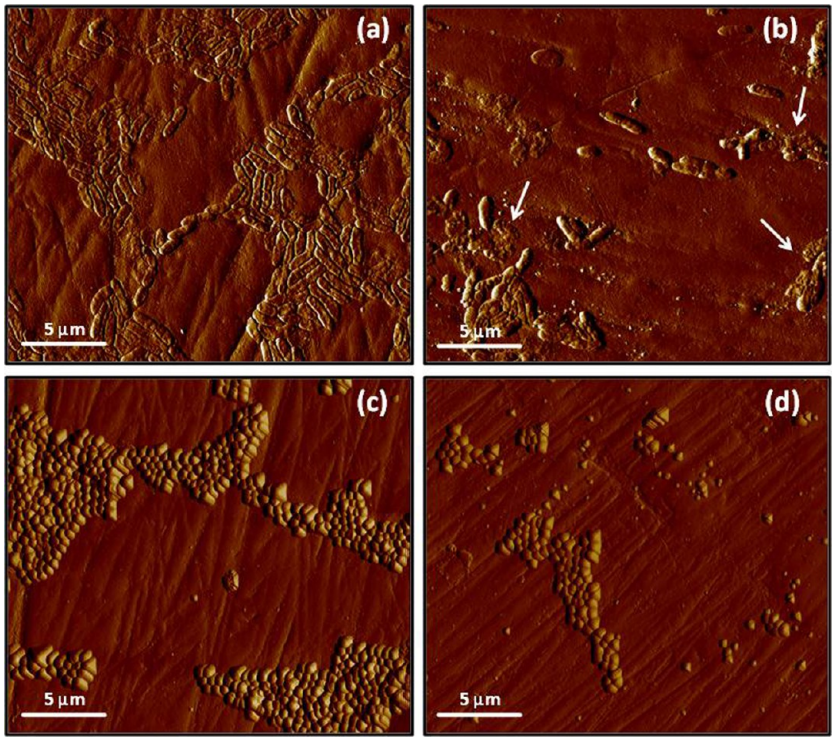

Figure 5. Contact-mode AFM images (deflection error) of early stages of biofilm formation: (a) *P. aeruginosa* on Ti substrate; (b) *P. aeruginosa* on AgNP-Ti substrate. Arrows point out EPS: (c) *S. aureus* on Ti substrate; (d) *S aureus* on AgNP-Ti substrate.

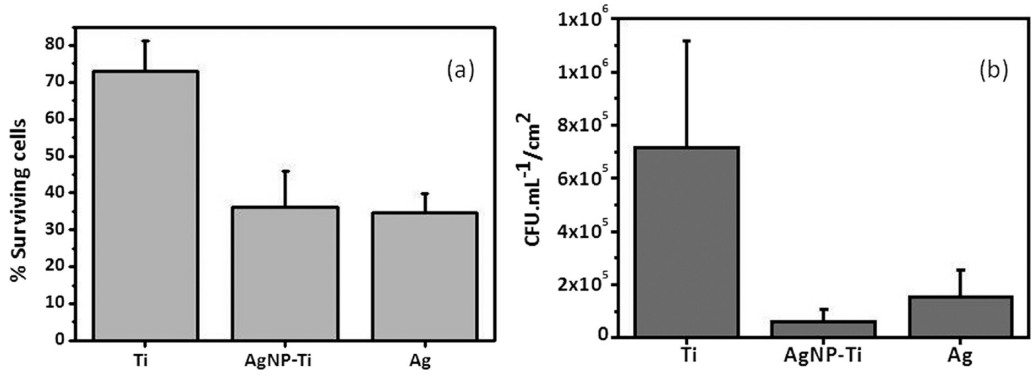

Figure 6. (a) Area covered by surviving *P. aeruginosa* related to the total area of the different substrates (Ti, AgNP-Ti, and Ag). (b) Viable *P. aeruginosa* obtained from the plate count method.

for the GMP medium, indicating that the culture medium itself is not significantly interfering with Ag species.

Antibacterial Effect of Adsorbed AgNPs on Ti. The antibacterial effect of adsorbed AgNPs was investigated for early stages of biofilm formation, i.e., after adhesion of bacteria forming two-dimensional aggregates and before development of the three-dimensional structure of the biofilm, in order to analyze the viability of pioneer bacteria. AgNP-Ti were exposed to either *P. aeruginosa* or *S. aureus* (1×10^8 CFU/mL). Bulk Ag foils and Ti substrates free of AgNPs (Ti) were exposed to the same cultures and used for comparison and as controls, respectively.

Figures 3a−c and 4a−c show representative epifluorescence images of cells attached on different substrates, where the organization and density of bacteria forming the biofilm can be observed. A comparison of the images shows that, as a general trend, bacteria attached on the control surface to a greater extent than on the Ag-containing substrates (AgNP-Ti and Ag) for both *P. aeruginosa* and *S. aureus*. It can be observed that *P. aeruginosa* organizes on Ti samples, mainly forming raftlike aggregates with some isolated bacteria spread on the surface. In contrast, on AgNP-Ti substrates, cells are more dispersed, and only a few attempts to form aggregates can be observed, while on Ag substrates only isolated cells can be detected (Figure 3). A closer picture of the bacterial organization for *P. aeruginosa* on both Ti and AgNP-Ti surfaces is shown in the contact-mode AFM images in Figure 5a,b. In the case of *S. aureus*, some aggregates are observed on Ti (Figures 4a and 5c). Conversely, on the AgNP-Ti substrates, isolated cells and a few small aggregates are formed (Figures 4b and 5d), while on Ag surfaces, only isolated bacteria are found (Figure 4c).

Semiquantitative analysis of the coverage on each surface was made from the epifluorescence images by measuring the total area covered by cells and referring the value to the area of the image (eq 2).

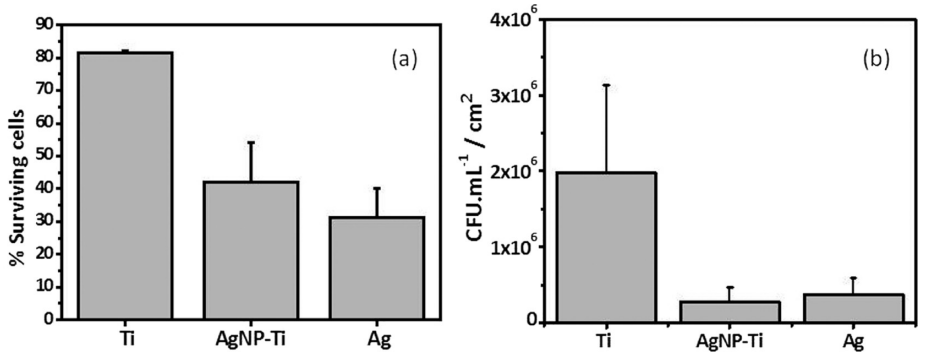

Figure 7. (a) Area covered by surviving *S. aureus* related to the total area of the different substrates (Ti, AgNP-Ti, and Ag). (b) Viable *S. aureus* obtained from the plate count method.

$$\%\text{adhesion} = \frac{\text{area covered by bacteria}}{\text{area of the image}} \times 100 \quad (2)$$

Figures 3d and 4d show average values of % adhesion for *P. aeruginosa* and *S. aureus*, respectively. It can be seen that AgNP-Ti and Ag substrates slightly inhibit the adhesion of cells, although the differences are not significant ($p < 0.05$) compared to the control Ti surfaces (Figures 3 and 4).

Epifluorescence images, obtained by staining the substrates with the Live/Dead kit, allow one to analyze sessile surviving bacteria compared to the total of bacteria (dead + surviving) attached to the same substrate. Thus, the percent of surviving cells was calculated following eq 3:

$$\%\text{surviving cells} = \frac{\text{area covered by surviving bacteria}}{\text{area covered by surviving and dead bacteria}} \times 100 \quad (3)$$

Analysis of sessile surviving bacteria on AgNP-Ti and Ag reveals that for both *P. aeruginosa* (Figure 6a) and *S. aureus* (Figure 7a) the area covered by surviving cells is lower than that for control Ti. The differences in percent of surviving cells between control Ti and Ag-containing substrates are significant ($p < 0.05$) for the two bacterial strains analyzed.

Quantitative analysis of viable bacteria was made by plate count. The CFU/mL values were referred to the area of each substrate. As expected from epifluorescence data, the presence of AgNPs on the Ti substrate reduced the number of viable bacteria for both *P. aeruginosa* and *S. aureus* compared to the controls. The number of CFU/mL of sessile *P. aeruginosa* on the different substrates is presented in Figure 6b. The CFU/(mL/cm^2) found on AgNP-free Ti was $7 \times 10^5 \pm 4 \times 10^5$, 1 order higher than those corresponding to AgNP-Ti ($6 \times 10^4 \pm 4 \times 10^4$ CFU/(mL/cm^2)) and 3-fold larger than the value observed for bulk Ag ($2 \times 10^5 \pm 1 \times 10^5$ CFU/(mL/cm^2)). A similar trend was found for *S. aureus*, as depicted in Figure 7b: after detachment of the cells, $2 \times 10^6 \pm 1 \times 10^6$ CFU/(mL/cm^2) were found on Ti, while only $3 \times 10^5 \pm 2 \times 10^5$ and $4 \times 10^5 \pm 2 \times 10^5$ CFU/(mL/cm^2) were found on AgNP-Ti and Ag, respectively. For both *P. aeruginosa* and *S. aureus*, significant differences ($p < 0.05$) between Ti and AgNP-Ti and Ti and Ag were found; i.e., the values decreased approximately 1 order in relation to bacteria attached to the control substrates. Also, for both strains, the number of viable bacteria attached to Ag substrates did not differ significantly ($p < 0.05$) to those found on AgNP-Ti. Thus, it can be concluded that AgNPs adsorbed on Ti reduced the number of viable bacteria at values that are comparable to those of bulk Ag.

It is worth mentioning that the larger amount of surviving bacteria found by epifluorescence assays compared to plate counting can be attributed to the technique itself. In fact, the Live/Dead kit utilizes a mixture of two dyes, SYTO 9 and propidium iodide, which have different abilities to penetrate the bacteria cell wall: the SYTO 9 fluorophore stains all bacteria green (those with intact membranes and those with damaged membranes), while propidium iodide penetrates only bacteria with damaged membranes, staining them red.[54] However, under certain conditions, cells with undamaged membranes are unable to duplicate and then the number of bacteria obtained by subtracting "red cells" from "green cells" account for both nonviable live (which may not duplicate) and viable (which can duplicate) bacteria. In contrast, the plate count reveals only viable bacteria. Thus, although the cell wall of some bacteria remains intact after being exposed to the Ag-containing surfaces, the number of bacteria capable of replicating and hence able to form the biofilm is only a fraction of the live bacterial population.

Interestingly, although both bacteria adhered to a similar extent on the three substrates (see Figures 4 and 5), as revealed by ANOVA analysis, the amount of viable bacteria on AgNP-Ti and Ag are significantly lower than that of the control, suggesting that a small amount of Ag (as in the nanoparticles, compared to bulk Ag) is enough to prevent formation of the biofilms. Indeed, from AFM images, the AgNP agglomerates are on average ~200 nm diameter and ~80 nm height, and its coverage from AFM and XPS results is 0.09.[30] This yields a total amount of Ag on the Ti substrate of $\sim 7 \times 10^{-8}$ mol of Ag/cm^2, which is small compared to pure Ag substrates. However, small nanoparticles can comparatively release a greater amount of ions than a planar surface because of the high area-to-volume ratio, the presence of surface defects, etc. In fact, the number of Ag atoms exposed to the medium is, at least, $\sim 2.3 \times 10^{14}$ atoms/cm^2, less than 10 times lower than that expected for polycrystalline Ag ($\sim 1 \times 10^{15}$ atoms/cm^2).

Additionally, we have measured the Ag ion release in water at 4 h for Ag foils and AgNP-Ti substrates. We have found that the Ag concentrations are 0.06 mg/L (0.55 μM) and 0.05 mg/L (0.46 μM) for Ag foil and AgNP-Ti substrate, respectively. The released Ag from the AgNP-Ti surface is 2.5% of the initial amount of adsorbed Ag.

Our results show that for 4 h practically the same Ag release is achieved from Ag and AgNP-Ti substrates, in agreement with the fact that the exposed Ag surface is very similar in both cases.

This explains why there are no significant differences in the number of sessile viable bacteria on both substrates.

Recalling our results for planktonic bacteria, these showed that *S. aureus* is more resistant to dispersed AgNPs than *P. aeruginosa*. However, when the same bacteria are attached on Ag-containing substrates, the susceptibility of both *P. aeruginosa* and *S. aureus* is similar because there is no significant difference in the number of viable cells counted for both strains. On this regard, AFM images of cells adhered on the AgNP-Ti showed some EPS around cells for the case of *P. aeruginosa* (see arrows in Figure 5 b), while its presence was not evident for *S. aureus.* In the case of *P. aeruginosa*, EPS production constitutes one of several steps in the development of biofilms,[51] having distinct roles, such as subpopulation interactions, macrocolony formation in the later stages of biofilm formation,[55] and antibiotic resistance.[56] Also, we have previously reported that EPS production is enhanced when cells adhere to toxic surfaces,[57] as a means to prevent contact with the aggressive compounds released from the surface. EPS is a polymeric conglomeration mainly composed of extracellular polysaccharides and proteins. Among polysaccharides, alginate, *Pel*, and *Psl* have been identified in *P. aeruginosa* EPS, and all of them have been associated with biofilm development and resistance to antimicrobials.[58] Indeed, the production of such polysaccharides seems to be responsible for the resistance of biofilmed bacteria to cationic antibiotics such as aminoglycosides through electrostatic interactions that entrap the antimicrobial into the negatively charged alginate and *Pel*.[58] Accordingly, the EPS excreted by adhered *P. aeruginosa* cells on AgNP-Ti surfaces could trap positively charged Ag^I ions and, as a consequence, the susceptibility of pioneer *P. aeruginosa* to AgNPs would diminish compared to planktonic bacteria,[2] rendering it similar to that of *S. aureus* in biofilms, which have not evidenced EPS production on those substrates.

Notably, when individual bacterial surfaces were analyzed, an important change in the bacterial cell-wall morphology was evidenced in the case of *P. aeruginosa* after 4 h of colonization on AgNP-Ti substrates (Figure 8a) compared to those attached on Ti surfaces (Figure 8b). The morphology of *P. aeruginosa* on control surfaces revealed intact cells, featuring undamaged walls, indicating that Ti itself does not produce changes in the bacterial morphology (Figure 8a). In contrast, some of the bacteria attached to AgNP-Ti substrates show some kind of membrane disruption, evidenced as an irregular surface (Figure 8b). In order to more thoroughly evaluate this change in surface features, the average roughness (w) of the bacterial surfaces was calculated. The values corresponding to Ti and AgNP-Ti substrates, calculated according to eq 1 (see the Experimental Section), are 9.4 and 19.0 nm, respectively (measured from images 450 × 450 nm^2 in size). Thus, the roughness of the walls of bacteria attached to AgNP-Ti substrates was twice that found for control Ti substrates. These findings can be appreciated in the AFM images shown in Figure 8.

In relation to this, it is well-known that antimicrobials cause morphological (size and shape) and surface (roughness and disruption) alterations in bacteria. The degree of damage depends on the concentration and incubation time of antimicrobial treatment.[59] Related to this, similar changes in the roughness of the cell surface as a consequence of exposure to different concentrations of antibiotic[60] and other biocides[60,61] have been reported. In the present study, the increase in the roughness of the cell wall was only observed on *P. aeruginosa* adhered on AgNP-Ti substrates, while it was not evident in the cell walls of *S. aureus* (data not shown). Alterations in the cell membrane caused by Ag ions and AgNPs were reported when uncoated and glutathione-coated AgNPs were grafted on glass and exposed to *E. coli* cultures.[15]

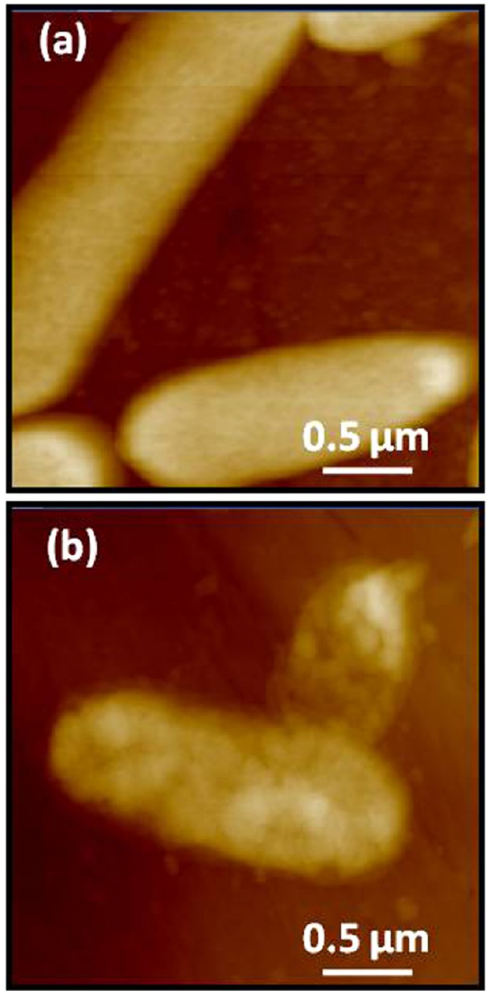

Figure 8. AFM images of *P. aeruginosa* attached to (a) control Ti substrate and (b) AgNP-Ti substrate.

In our case, an increase in the cell-wall roughness due to the adsorption of AgNPs would imply detachment of the adsorbed AgNPs from the Ti substrate. However, the stability of the adsorbed AgNPs is relatively strong because high forces (≈400 nN) are necessary to sweep away some of the adsorbed nanoparticles (data not shown). Thus, it is improbable that the increase of the roughness is due to the detachment of AgNPs from the substrate and the subsequent attachment on the cell wall.

Membrane disruption due to the release of Ag^I ions and nanoparticle internalization was found on Gram-negative bacteria, while Gram-positive bacteria (*S. aureus*) remained unchanged after Ag treatment. This can be due to the fact that the cellular membrane in Gram-negative cells contains thiol-bearing proteins and phospholipids, which present high affinity for Ag species.[15,62] Thus, here also we can interpret that the less rigid membrane of Gram-negative bacteria is more active to Ag, irrespective of the mechanism of action, either release of Ag^I ions or short-distance nanomechanical action due to nanoparticle internalization.

CONCLUSIONS

We have analyzed the effect of free and immobilized AgNPs on both Gram-positive and Gram-negative bacteria. Regarding free AgNPs, the MBC found for *P. aeruginosa* was lower than that for *S. aureus*. The higher susceptibility of Gram-negative bacteria can be interpreted in terms of their less rigid cell-wall structure, which is more active to Ag irrespective of the mechanism of action [either the release of Ag^I ions or nanoparticle internalization]. Thus, the role of the cell-wall structure would be crucial in the antibacterial action of AgNPs. Further investigation is needed in order to completely elucidate this point. The MBC corresponding to small (≈6 nm diameter), citrate-capped AgNPs for both strains is much lower than those reported in the literature for different diameters and capping. Moreover, because the minimum concentration of Ag at which AgNPs are cytotoxic to osteoblasts is much higher than that necessary to kill bacteria, these nanoparticles can be used with no detrimental effect on the cells. Therefore, we can conclude that there would be a concentration window that allows the use of AgNPs as antibacterial agents without damaging the cells in the vicinity of the implants.

In relation to bone implants, AgNPs adsorbed on Ti/TiO_2 have proven to be effective to prevent biofilm formation for both Gram-positive and Gram-negative bacteria. The fact that AgNP-Ti and Ag substrates have similar bactericidal effects for sessile *P. aeruginosa* and *S. aureus* while, for planktonic bacteria, *P. aeruginosa* is more affected than *S. aureus* could be explained by the additional protection that the EPSs (only present for *P. aeruginosa*) give to the cells present in the biofilm. The small amount of Ag on the surface of Ti has an antimicrobial effect similar to that of bulk Ag. This result is important to improve the performance of Ti-made implantable devices: the good mechanical properties and the biocompatibility of Ti are maintained, and bacteria colonization is prevented because of the fact that AgNPs on Ti show an antimicrobial activity similar to that of bulk Ag, with only a small amount of Ag on the surface. Moreover, because the method involved in the adsorption of AgNPs on Ti is easy and inexpensive, it could be implemented in the clinical environment.

AUTHOR INFORMATION

Corresponding Author

*E-mail: cvericat@inifta.unlp.edu.ar (C.V.), pls@inifta.unlp.edu.ar (P.L.S.).

Notes

The authors declare no competing financial interest.

ACKNOWLEDGMENTS

The authors are grateful to CONICET (PIP 0362), UNLP (11/X532), and ANPCyT (PICT 2010-1779, PICT 2010-2554, and PPL 2011-003) for financial support. C.Y.F. and A.G.M. acknowledge fellowships from CONICET. The authors also thank Dr. Mónica Fernández Lorenzo for her helpful comments.

REFERENCES

(1) Zhao, L.; Chu, P. K.; Zhang, Y.; Wu, Z. *J. Biomed. Mater. Res., Part B* **2009**, *91B*, 470−480.
(2) Wirth, S. M.; Lowry, G. V.; Tilton, R. D. *Environ. Sci. Technol.* **2012**, *46*, 12687−12696.
(3) Lara, H.; Garza-Trevino, E.; Ixtepan-Turrent, L.; Singh, D. *J. Nanobiotechnol.* **2011**, *9*, 30.
(4) Kim, K.-J.; Sung, W. S.; Moon, S.-K.; Choi, J.-S.; Kim, J. G.; Lee, D. G. *J. Microbiol. Biotechnol.* **2008**, *18*, 1482−1484.
(5) Yliniemi, K.; Vahvaselka, M.; Ingelgem, Y. V.; Baert, K.; Wilson, B. P.; Terryn, H.; Kontturi, K. *J. Mater. Chem.* **2008**, *18*, 199−206.
(6) Pallavicini, P.; Taglietti, A.; Dacarro, G.; Diaz-Fernandez, Y. A.; Galli, M.; Grisoli, P.; Patrini, M.; Santucci De Magistris, G.; Zanoni, R. *J. Colloid Interface Sci.* **2010**, *350*, 110−116.
(7) Chernousova, S.; Epple, M. *Angew. Chem., Int. Ed.* **2013**, *52*, 1636−1653.
(8) Vasilev, K.; Sah, V. R.; Goreham, R. V.; Ndi, C.; Short, R. D.; Griesser, H. J. *Nanotechnology* **2010**, *21*, 215102.
(9) Zaporojtchenko, V.; Podschun, R.; Schürmann, U.; Kulkarni, A.; Faupel, F. *Nanotechnology* **2006**, *17*, 4904.
(10) Lee, H. Y.; Park, H. K.; Lee, Y. M.; Kim, K.; Park, S. B. *Chem. Commun.* **2007**, *0* (28), 2959−2961.
(11) Sivolella, S.; Stellini, E.; Brunello, G.; Gardin, C.; Ferroni, L.; Bressan, E.; Zavan, B. *J. Nanomater.* **2012**, Article ID 975842, 12 pages.
(12) Holt, K. B.; Bard, A. J. *Biochemistry* **2005**, *44*, 13214−13223.
(13) Liu, J.; Hurt, R. H. *Environ. Sci. Technol.* **2010**, *44*, 2169−2175.
(14) Sotiriou, G. A.; Pratsinis, S. E. *Environ. Sci. Technol.* **2010**, *44*, 5649−5654.
(15) Taglietti, A.; Diaz Fernandez, Y. A.; Amato, E.; Cucca, L.; Dacarro, G.; Grisoli, P.; Necchi, V.; Pallavicini, P.; Pasotti, L.; Patrini, M. *Langmuir* **2012**, *28*, 8140−8148.
(16) Wu, J.; Hou, S.; Ren, D.; Mather, P. T. *Biomacromolecules* **2009**, *10*, 2686−2693.
(17) Xiu, Z.-m.; Zhang, Q.-b.; Puppala, H. L.; Colvin, V. L.; Alvarez, P. J. J. *Nano Lett.* **2012**, *12*, 4271−4275.
(18) Hwang, E. T.; Lee, J. H.; Chae, Y. J.; Kim, Y. S.; Kim, B. C.; Sang, B. I.; Gu, M. B. *Small* **2008**, *4*, 746−750.
(19) Ansari, M.; Khan, H.; Khan, A.; Malik, A.; Sultan, A.; Shahid, M.; Shujatullah, F.; Azam, A. *Biol. Med.* **2011**, *3*, 141−146.
(20) Lara, H.; Ayala-Núñez, N.; Ixtepan Turrent, L.; Rodríguez Padilla, C. *World J. Microbiol. Biotechnol.* **2010**, *26*, 615−621.
(21) Amato, E.; Diaz-Fernandez, Y. A.; Taglietti, A.; Pallavicini, P.; Pasotti, L.; Cucca, L.; Milanese, C.; Grisoli, P.; Dacarro, C.; Fernandez-Hechavarria, J. M.; Necchi, V. *Langmuir* **2011**, *27*, 9165−9173.
(22) Pal, S.; Tak, Y. K.; Song, J. M. *Appl. Environ. Microbiol.* **2007**, *73*, 1712−1720.
(23) Martínez-Castañón, G.; Niño-Martínez, N.; Martínez-Gutierrez, F.; Martínez-Mendoza, J.; Ruiz, F. *J. Nanopart. Res.* **2008**, *10*, 1343−1348.
(24) Levard, C.; Hotze, E. M.; Lowry, G. V.; Brown, G. E. *Environ. Sci. Technol.* **2012**, *46*, 6900−6914.
(25) Elias, C. N.; Lima, J. H. C.; Valiev, R.; Meyers, M. A. *JOM* **2008**, *60*, 46−49.
(26) Willie, B. M.; Yang, X.; Kelly, N. H.; Merkow, J.; Gagne, S.; Ware, R.; Wright, T. M.; Bostrom, M. P. G. *J. Biomed. Mater. Res., Part A* **2010**, *92B*, 479−488.
(27) Juan, L.; Zhimin, Z.; Anchun, M.; Lei, L.; Jingchao, Z. *Int. J. Nanomed.* **2010**, *5*, 261−267.
(28) Secinti, K. D.; Özalp, H.; Attar, A.; Sargon, M. F. *J. Clin. Neurosci.* **2011**, *18*, 391−395.
(29) Roe, D.; Karandikar, B.; Bonn-Savage, N.; Gibbins, B.; Roullet, J.-B. *J. Antimicrob. Chemother.* **2008**, *61*, 869−876.
(30) Flores, C. Y.; Diaz, C.; Rubert, A.; Benítez, G. A.; Moreno, M. S.; Fernández Lorenzo de Mele, M. A.; Salvarezza, R. C.; Schilardi, P. L.; Vericat, C. *J. Colloid Interface Sci.* **2010**, *350*, 402−408.
(31) de Lima, R.; Seabra, A. B.; Durán, N. *J. Appl. Toxicol.* **2012**, *32*, 867−879.
(32) Kim, S.; Choi, J. E.; Choi, J.; Chung, K.-H.; Park, K.; Yi, J.; Ryu, D.-Y. *Toxicol. In Vitro* **2009**, *23*, 1076−1084.
(33) Hackenberg, S.; Scherzed, A.; Kessler, M.; Hummel, S.; Technau, A.; Froelich, K.; Ginzkey, C.; Koehler, C.; Hagen, R.; Kleinsasser, N. *Toxicol. Lett.* **2011**, *201*, 27−33.

(34) Gongadze, E.; Kabaso, D.; Bauer, S.; Slivnik, T.; Schmuk, i. P.; van Rienen, U.; Iglič, A. *Int. J. Nanomed.* **2011**, *6*, 1801−1816.
(35) Sul, Y.-T. *Biomaterials* **2003**, *24*, 3893−3907.
(36) Gorth, D. J.; Puckett, S.; Ercan, B.; Webster, T. J.; Rahaman, M.; Sonny Bal, B. *Int. J. Nanomed.* **2012**, *7*, 4829−4840.
(37) Bjerkan, G.; Witso, E.; Bergh, K. *Acta Orthop.* **2009**, *80*, 245−50.
(38) Ceri, H.; Olson, M. E.; Stremick, C.; Read, R. R.; Morck, D.; Buret, A. *J. Clin. Microbiol.* **1999**, *37*, 1771−1776.
(39) Brooun, A.; Liu, S.; Lewis, K. *Antimicrob. Agents Chemother.* **2000**, *44*, 640−6.
(40) Borenfreund, E.; Puerner, J. A. *Toxicol. Lett.* **1985**, *24*, 119−124.
(41) Mosmann, T. *J. Immunol. Methods* **1983**, *65*, 55−63.
(42) Twentyman, P. R.; Luscombe, M. *Br. J. Cancer* **1987**, *56*, 279−285.
(43) Morones, J. R.; Elechiguerra, J. L.; Camacho, A.; Holt, K.; Kouri, J. B.; Ramirez, J. T.; Yacaman, M. J. *Nanotechnology* **2005**, *16*, 2346−2353.
(44) Jain, J.; Arora, S.; Rajwade, J. M.; Omray, P.; Khandelwal, S.; Paknikar, K. M. *Mol. Pharm.* **2009**, *6*, 1388−1401.
(45) Panáček, A.; Kvítek, L.; Prucek, R.; Kolář, M.; Večeřová, R.; Pizúrová, N.; Sharma, V. K.; Nevěčná, T. j.; Zbořil, R. *J. Phys. Chem. B* **2006**, *110* (33), 16248−16253.
(46) Li, X.; Lenhart, J. J. *Environ. Sci. Technol.* **2012**, *46*, 5378−5386.
(47) Verma, A.; Stellacci, F. *Small* **2010**, *6*, 12−21.
(48) Feng, Q. L.; Wu, J.; Chen, G. Q.; Cui, F. Z.; Kim, T. N.; Kim, J. O. *J. Biomed. Mater. Res.* **2000**, *52*, 662−668.
(49) Elechiguerra, J. L.; Larios-Lopez, L.; Liu, C.; Garcia-Gutierrez, D.; Camacho-Bragado, A.; Yacaman, M. J. *Chem. Mater.* **2005**, *17*, 6042−6052.
(50) Eckhardt, S.; Brunetto, P. S.; Gagnon, J.; Priebe, M.; Giese, B.; Fromm, K. M. *Chem. Rev.* **2013**, DOI: 10.1021/cr300288v.
(51) Renner, L. D.; Weibel, D. B. *MRS Bull.* **2011**, *36*, 347−355.
(52) Carlson, C.; Hussain, S. M.; Schrand, A. M.; Braydich-Stolle, L. K.; Hess, K. L.; Jones, R. L.; Schlager, J. J. *J. Phys. Chem. B* **2008**, *112*, 13608−13619.
(53) AshaRani, P. V.; Low Kah Mun, G.; Hande, M. P.; Valiyaveettil, S. *ACS Nano* **2008**, *3*, 279−290.
(54) http://tools.invitrogen.com/content/sfs/manuals/mp07007.pdf.
(55) Yang, L.; Hu, Y.; Liu, Y.; Zhang, J.; Ulstrup, J.; Molin, S. *Environ. Microbiol.* **2011**, *13*, 1705−1717.
(56) Ryder, C.; Byrd, M.; Wozniak, D. J. *Curr. Opin. Microbiol.* **2007**, *10*, 644−648.
(57) Díaz, C.; Schilardi, P.; Fernández Lorenzo de Mele, M. *Artif. Organs* **2008**, *32*, 292−298.
(58) Colvin, K. M.; Gordon, V. D.; Murakami, K.; Borlee, B. R.; Wozniak, D. J.; Wong, G. C. L.; Parsek, M. R. *PLoS Pathog.* **2011**, *7*, e1001264.
(59) Mangalappalli-Illathu, A. K.; Vidovic, S.; Korber, D. R. *Antimicrob. Agents Chemother.* **2008**, *52*, 3669−3680.
(60) Nikiyan, H.; Vasilchenko, A.; Deryabin, D. *AFM investigations of Various Disturbing Factors on Bacterial Cells*; Formatex Research Center: Badajoz, 2010; Vol. *1*, pp 523−529.
(61) Deupree, S. M.; Schoenfisch, M. H. *Acta Biomater.* **2009**, *5*, 1405−1415.
(62) Li, W.-R.; Xie, X.-B.; Shi, Q.-S.; Zeng, H.-Y.; Ou-Yang, Y.-S.; Chen, Y.-B. *Appl. Microbiol. Biotechnol.* **2010**, *85*, 1115−1122.